Available online at www.sciencedirect.com

ScienceDirect

IFAC PapersOnline CONFERENCE PAPER ARCHIVE

IFAC PapersOnLine 52-28 (2019) 126–133

Continuous Identification of Driver Model Parameters via the Unscented Kalman Filter

Yishen Zhao*. Philippe Chevrel*. Fabien Claveau*. Franck Mars.**

** IMT Atlantique, LS2N UMR CNRS 6004 (Laboratoire des Sciences du Numérique de Nantes), 44307 Nantes, France (e-mails: firstname.lastname@ls2n.fr)*
*** CNRS & Centrale Nantes, LS2N UMR CNRS 6004 (Laboratoire des Sciences du Numérique de Nantes), 44321 Nantes, France, (e-mail: firstname.lastname@ls2n.fr)}*

Abstract: Advanced Driver-Assistance Systems (ADAS) have become an essential part of modern cars. Among the solutions proposed, haptic shared control of the steering wheel is increasingly being studied. A fundamental question is how drivers adapt their behavior to these systems. This article proposes to use the Unscented Kalman Filter (UKF) to identify the variation over time in the psychological and neuromuscular parameters of a driver structured model. The goal here is to understand how the driver adapts to changes, whether regarding the behavior of the steering system, the visibility or the road conditions. The LPV system considered for identification is known as the cybernetic driver model. Two experiments carried out respectively with Simulink© and on a driving simulator provide the data. The methodology proposed for tuning the UKF is studied from the results obtained with those data. A multi-UKF strategy is also considered. The methodology reveals useful when a compromise between rapidity and precision has to be achieved for parameters estimation. It opens the way to a detailed analysis of the driver's parameter variations within the multi-UKF framework.

Keywords: Driver Model, LPV Identification, Unscented Kalman Filter, Kalman Filter Tuning

1. INTRODUCTION

Modern cars are more and more equipped with Advanced Driver-Assistance Systems (ADAS). For example, the Lane Departure Avoidance (LDA) systems warn the driver when the vehicle begins to move out of its lane unless a turn signal is on in that direction. The Lane Keeping Support (LKS) or lane centring systems help driver stay in the lane relieving driver of the steering task. Such systems either warn the driver in a critical situation, like the LDA, or take over full control of a subtask like the LKS. When steering is fully automated, the human driver will act like a supervisor of the system and monitors unexpected changes. As a consequence, the driver is out of the perceptual-motor loop, without any direct feedback from the steering wheel (Mole et al., 2019).

An alternative approach, haptic "shared control" has been proposed (Abbink et al., 2012; Mark Mulder et al., 2012). In shared control, both human driver and automation interact through the steering wheel, which continuously provides feedback of the system actions. In addition, the human can override the system or give way to it, if it is safe and necessary to do so (Steele & Gillespie, 2001). Haptic shared control driver-assistance systems have shown their advantages in improvement of driver's objective performance (Flad et al., 2017) and become an increasingly popular approach to facilitate control and communication between human and intelligent machines.

One of the fundamental questions in the development and implementation of haptic shared control systems concerns how the action of driver-assistance systems can smoothly take part in the driver's sensorimotor loop. Incorporating a cybernetic driver model in the controller design has been proposed as a solution (Mars & Chevrel, 2017; Mars et al., 2011; Saleh et al., 2013, 2011). This approach allows to take into account the predictions of the driver model to improve human-machine cooperation.

Another open question related to the design of haptic shared control systems is how to consider the driver potential adaption to the system. Adaptation may be due to the prolonged use of the system (Mars, Deroo, & Charron, 2014) or to variations in the environment (Mars, Deroo, & Hoc, 2014), for instance. This may be achieved by adaptation of the driver model parameters as a function of time or conditions. The present paper aims to evaluate a method to achieve this goal.

Previous interdisciplinary researches focusing on the estimation of driver's distraction (Ameyoe et al., 2015) showed that one possible methodology is identifying in real-time the variation of perceptual and neuromuscular parameters in a driver cybernetic model. Since the parameters in the driver model are varying, this approach is actually dealing with a Linear Parameter-Varying (LPV) system identification problem.

10.1016/j.ifacol.2019.12.359

To deal with the driver's adaptation process to different changes in his or her driving environment, this article adopts the idea of using the Unscented Kalman Filter (UKF) to identify an embedded driver model. The tuning methodology will be emphasized and a multi-UKF approach will be proposed. The method is validated through experiments. In section 2, the parametrized cybernetic driver model is presented. Section 3 implements the identification method based on UKF, section 4 discusses its tuning methodology and proposes a practical approach. Section 5 shows results of two experiments to validate the method, one with simulation data and another with experimental data from a driving simulator. Section 6 summarizes general conclusions.

2. CYBERNETIC DRIVER MODEL

The principle of a cybernetic driver model is based on a "perception-action" cycle which represents perceptual and motor processes (Max Mulder et al., 2004). The development of such models originates from human operator model in aeronautics (McRuer et al., 1977) during the 1950s. (Donges, 1978) proposed a seminal two-level model for vehicle control with anticipatory open loop control and compensatory closed loop control. During the 1980s and 1990s, human physical attributes and neuromuscular system were taken into consideration (Hess & Modjtahedzadeh, 1990). A visual control model of steering has been proposed later (Salvucci & Gray, 2004). In an effort to integrate all those models, a new model has been proposed (Mars & Chevrel, 2017; Mars et al., 2011; Saleh et al., 2011). It represents the driver's visual behaviour as the processing of two points on the road, a far point and a near point. The near point is used to compensate for lateral position errors while the far point is used to anticipate the road ahead. The visual information is then processed with a neural delay before feeding to the neuromuscular model. The neuromuscular action is modelled based on neurophysiology (Hoult & Cole, 2008). The block diagram of the cybernetic driver model is shown in Fig. 1.

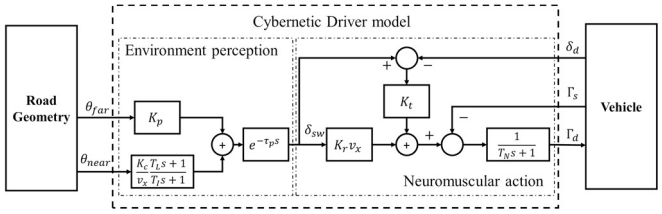

Fig. 1 Cybernetic driver model

Signals and parameters are described in Table 1 and Table 2.

Table 1 Description of signals in driver model

Signal	Description
θ_{far}	Visual anticipation angle
θ_{near}	Visual compensation angle
δ_d	Steering wheel angle
Γ_s	Self-aligning torque
Γ_d	Driver steering wheel torque
δ_{SW}	Driver intention of steering wheel angle

Table 2 Description of parameters in driver model

Parameter	Description	Normal value
K_p	Visual anticipation gain	3.4
K_c	Visual compensation gain	15
T_I, T_L	Compensation time constant	1, 3
τ_p	Processing delay	0.04
K_r	Internal gain of steering column stiffness	1
K_t	Gain of stretch reflex	12
T_N	Neuromuscular time constant	0.1
v_x	Vehicle longitudinal velocity	18

The delay can be approximated by using 1st order Padé model:

$$e^{-\tau_p s} \approx \frac{1 - 0.5\tau_p s}{1 + 0.5\tau_p s} \tag{1}$$

The minimal realization of the cybernetic driver model depicted in Fig.1 could be written as follows.

$$\begin{cases} \dot{x}(t) = A(\Theta)x(t) + B(\Theta)u(t) + w(t) \\ y(t) = C(\Theta)x(t) + D(\Theta)u(t) + v(t) \end{cases} \tag{2}$$

where:

Input $u(t) = [\theta_{far} \quad \theta_{near} \quad \delta_d \quad \Gamma_s]^T$;

Output $y(t) = [\Gamma_d \quad \delta_{sw}]^T$;

Parameters $\Theta(t) = [K_p \quad K_c \quad T_I \quad T_L \quad \tau_p \quad K_r \quad K_t \quad T_N]^T$;

$$A(\Theta) = \begin{bmatrix} -\frac{1}{T_I} & 0 & 0 \\ \frac{K_c}{v_x}\frac{2}{\tau_p}\left(1 - \frac{T_L}{T_I}\right) & -\frac{2}{\tau_p} & 0 \\ -\frac{K_r v_x + K_t}{T_N}\frac{K_c}{v_x}\left(1 - \frac{T_L}{T_I}\right) & 2\frac{K_r v_x + K_t}{T_N} & -\frac{1}{T_N} \end{bmatrix}$$

$$B(\Theta) = \begin{bmatrix} 0 & \frac{1}{T_I} & 0 & 0 \\ K_p\frac{2}{\tau_p} & \frac{K_c}{v_x}\frac{2}{\tau_p}\frac{T_L}{T_I} & 0 & 0 \\ -K_p\frac{K_r v_x + K_t}{T_N} & -\frac{K_r v_x + K_t}{T_N}\frac{K_c}{v_x}\frac{T_L}{T_I} & -\frac{K_t}{T_N} & -\frac{1}{T_N} \end{bmatrix}$$

$$C(\Theta) = \begin{bmatrix} 0 & 0 & 1 \\ -\frac{K_c}{v_x}\left(1 - \frac{T_L}{T_I}\right) & 2 & 0 \end{bmatrix}$$

$$D(\Theta) = \begin{bmatrix} 0 & 0 & 0 & 0 \\ -K_p & -\frac{K_c}{v_x}\frac{T_L}{T_I} & 0 & 0 \end{bmatrix}$$

$w(t)$ and $v(t)$ are process noise and measurement noise, with respective covariance matrix Q_x and R.

3. PARAMETER IDENTIFICATION

Identification methods for LPV system have been intensively studied recently. For example, Tóth proposed an extension of the Refined Instrumental Variable (RIV) approach for closed

loop LPV systems (Tóth et al., 2011); Zhang discussed about the local approach by interpolating individually estimated local linear time invariant (LTI) models (Zhang & Ljung, 2017); Darwish introduced a nonparametric Gaussian regression approach based on prediction-error (Darwish et al., 2018); Rizvi presented another nonparametric method for state-space LPV model using kernelized machine learning (Rizvi et al., 2018). In this section a parametric method based on Unscented Kalman Filter is proposed. It is demonstrated that under certain hypothesis, the driver LPV model (2) can be rewritten as a non-linear system (3) (see below) by augmenting system states in (2) with parameter dynamics. It therefore turns the parameter identification problem of the LPV system (2) to a non-linear state estimation problem associated to system (3). Compared to methods previously pointed out, the one chosen has the possibility of 1) balancing the rapidity and sensitivity of identification via tuning the dynamics of the state observer and 2) defining the dynamic of parameters according to *a prior* knowledge on the nature of parameter variations such as continuity, derivability, time constant etc.

3.1 Augmented Model and State Estimation

Before rewriting the driver model as an augmented system, working hypothesis must be made to guarantee the conditions of utilizing Unscented Kalman Filter (UKF) for parameter identification.

Hypothesis 1: the driver model parameters are considered as time varying and are modelled as Wiener processes, i.e. $\dot{\Theta}(t) = w_\Theta(t)$ where $w_\Theta(t) \sim N(0, \sigma_\Theta^2)$, namely the $\Theta(t)$ is a Wiener process (scaling limit of a random walk), or a random walk itself in discrete time.

Actually, different kinds of stochastic process could be chosen for $w_\Theta(t)$ based on *a priori* knowledge of parameter dynamics. For example, if $w_\Theta(t)$ is a sum of several Dirac functions with random amplitude at random time, the $\Theta(t)$ is thus a piecewise constant signal.

Hypothesis 2: the variations of all parameters are slower than those of system states.

This hypothesis distinguishes, within the augmented system states defined below (see (3)), the variables predefined as "parameters" from the state variables as defined in (2). If the parameters evolved more rapidly than the system states, the linearization performed implicitly to design the Kalman Filter would be unjustified.

Under Hypothesis 1 & 2, the augmented system is defined as:

$$\begin{cases} \dot{x}_a(t) = f\big(x_a(t), u(t)\big) + w_a(t) \\ y(t) = g\big(x_a(t), u(t)\big) + v(t) \end{cases} \quad (3)$$

with

1) Augmented system states $x_a(t) = [x(t) \quad \Theta(t)]^T$
2) Augmented process noise $w_a(t) = [w(t) \quad w_\Theta(t)]^T$
3) Parameters' process noise covariance Q_Θ
4) Augmented process noise covariance Q_a
5) State-transition function

$$f\big(x_a(t), u(t)\big) = \begin{bmatrix} A(\Theta)x(t) + B(\Theta)u(t) \\ 0 \end{bmatrix}$$

6) Measurement function

$$g\big(x_a(t), u(t)\big) = C(\Theta)x(t) + D(\Theta)u(t)$$

A commonly used state estimator is the Luenberger observer. For the augmented system (3), such observer can be written as

$$\dot{\hat{x}}_a(t) = f\big(\hat{x}_a(t), u(t)\big) + L(t)\big[y(t) - g\big(\hat{x}_a(t), u(t)\big)\big] \quad (4)$$

where $L(t)$ is the observer gain. If the augmented system (3) is considered as a deterministic system without noise $w_a(t)$ and $v(t)$, an optimal observer gain for state estimation, which is also the Kalman gain, can be obtained by minimizing the cost function (5).

$$\begin{aligned} J\big(\hat{x}_{a,0}, \hat{x}_a\big) &= \hat{x}_{a,0}^T P_{a,0}^{-1} \hat{x}_{a,0} \\ &+ \int_0^{t_f} \big[\dot{\hat{x}}_a - f(x_a, u)\big]^T Q_a^{-1} \big[\dot{\hat{x}}_a - f(x_a, u)\big] dt \\ &+ \int_0^{t_f} [y - g(x_a, u)]^T R^{-1} [y - g(x_a, u)] dt \end{aligned} \quad (5)$$

where $P_{a,0}$, Q_a and R are respectively weighting matrices for initial states, state transitions and measurements in this case instead of covariance matrices. From this point of view, the dynamic of observer can thus be configured via tuning these weighting matrices.

In following sections, the LPV system states in (2) are still called as "system states" or just "states", except if it is explicitly pointed out to be "augmented system states". Same for "process noise" and "augmented process noise".

3.2 Discretization and Implementation via UKF

3.2.1 Discretization

For numerical calculation and implementation of UKF, the augmented system (3) needs to be discretized. With Euler's approximation the augmented system in discrete time becomes

$$\begin{cases} x_a[k+1] = f_d(x_a[k], u[k]) + w_{a,d}[k] \\ y[k] = g_d(x_a[k], u[k]) + v[k] \end{cases} \quad (6)$$

with

1) Discretized noise: $w_{a,d}[k] = T_s w_a(kT_s)$, $v[k] = v(kT_s)$
2) Noise covariance

$$Q_{a,d} = T_s Q_a, R_d = R/T_s$$

3) State-transition function

$$f_d(x_a[k], u[k]) = \begin{bmatrix} (T_s A(\Theta) + I)x[k] + T_s B(\Theta)u[k] \\ \Theta[k] \end{bmatrix}$$

4) Measurement function

$$g_d(x_a[k], u[k]) = C(\Theta)x[k] + D(\Theta)u[k]$$

where T_s is sample time, I is identity matrix.

The observer (4) is now considered in discrete time according to the discrete augmented system (6).

$$\begin{aligned} \hat{x}_a[k+1] = f_d(\hat{x}_a[k], u[k]) \\ + L[k]\big(y[k] - g_d(\hat{x}_a[k], u[k])\big) \end{aligned} \quad (7)$$

3.2.2 Unscented Transformation

In order to calculate the optimal Kalman gain $L[k]$ in (7), the Extended Kalman Filter (EKF) uses Jacobian matrices of

functions f and g. This is actually an approximation using a first-order Taylor series expansion to locally linearize the non-linear system. However, when high non-linearity appears, the computational complexity increases and result may be inaccurate (Wan et al., 2000). The Unscented Kalman Filter (UKF) utilizes the "Unscented Transformation" (UT) to calculate the statistical properties of a random variable that has undergone a nonlinear transformation (Julier & Uhlmann, 1997). Given a vector of random variables x of dimension N propagating through a non-linear function $z = h(x)$ with mean $\bar{x}$ and covariance C_{xx}, the statistics of z is calculated by Algorithm 1.

Algorithm 1: Unscented Transformation

Step 1: Sigma points

Form a matrix X of $2N + 1$ vectors. Each vector, called sigma point (in N dimension space), is calculated by

$$X_i = \begin{cases} \bar{x}, & i = 0 \\ \bar{x} + \left(\sqrt{NC_{xx}}\right)_i, & i = 1,2,\dots,N \\ \bar{x} - \left(\sqrt{NC_{xx}}\right)_{i-N}, & i = N+1, N+2,\dots,2N \end{cases} \quad (8)$$

where $\sqrt{NC_{xx}}$ is the square root matrix of NC_{xx} such that $\sqrt{NC_{xx}}\left(\sqrt{NC_{xx}}\right)^T = NC_{xx}$ and $\left(\sqrt{NC_{xx}}\right)_i$ is the ith column of $\sqrt{NC_{xx}}$.

Step 2: Propagated sigma points

The sigma points are propagated through the non-linear function h.

$$Z_i = h(X_i), i = 0,1,2,\dots,2N \quad (9)$$

Step 3: Mean and covariance of propagated sigma points

$$\bar{z} = \sum_{i=0}^{2N} W_i Z_i$$
$$C_{zz} = \sum_{i=0}^{2N} W_i (Z_i - \bar{z})(Z_i - \bar{z})^T \quad (10)$$

where W_i is a weighting factor.

Step 4: Cross-covariance between x and z

$$C_{xz} = \sum_{i=0}^{2N} W_i (X_i - \bar{x})(Z_i - \bar{z})^T \quad (11)$$

Adjustment of weighting factor W_i can improve the quality of approximation when the function h is highly non-linear. This is not the case here of the augmented system (3) that will be considered. So it is chosen hereafter $W_0 = 0$ and $W_i = \frac{1}{2N}$ $(i = 1,2,\dots,2N)$.

3.2.3 UKF Algorithm

The following Algorithm 2 details the calculation steps of UKF for estimating the augmented system states in system (6).

Algorithm 2: Unscented Kalman Filter

Step 1: Initialization

At time step $k = 0$, initialize augmented system states value $\hat{x}_a[0]$, augmented system states covariance matrix $P_a[0]$, augmented process noise covariance matrix $Q_{a,d}$ and measurement noise covariance matrix R_d.

Step 2: Calculation of the output prediction

At time step $k \geq 0$, estimate the output prediction using Unscented Transformation.

$$\left(\hat{y}[k|k-1], C'_{yy}[k], C_{xy}[k]\right) = UT(g_d, \hat{x}_a[k|k-1], P_a[k|k-1])$$

$$C_{yy}[k] = C'_{yy}[k] + R_d$$

Step 3: Correction with measurements

At time step k, correct the states estimated from the measurements, and the state covariance.

$$L[k] = C_{xy}[k] C_{yy}^{-1}[k]$$

$$\hat{x}_a[k|k] = \hat{x}_a[k|k-1] + L[k](y[k] - \hat{y}[k|k-1])$$

$$P_a[k|k] = P_a[k|k-1] - L[k] C_{xy}^T[k]$$

Step 4: Prediction of next step states' value

At time step k, predict system states (and the associated covariance) at next time step $k+1$ using Unscented Transformation.

$$(\hat{x}_a[k+1|k], P'_a[k+1|k]) = UT(f_d, \hat{x}_a[k|k], P_a[k|k])$$

$$P_a[k+1|k] = P'_a[k+1|k] + Q_{a,d}$$

Step 5: Increase one time step and repeat step 2 to 4 until the last time step.

4. PRATICAL USE OF UKF

4.1 UKF Tuning Methodology

Tuning, or initialisation is one of the common issues in using Kalman Filter. Some empirical conclusions in linear KF can be referred in UKF. As stated above, from a deterministic point of view, the dynamic of an optimal observer can be tuned via the weighting matrices $P_a[0], Q_{a,d}$ and R_d. From a stochastic point of view, the UKF will give an accurate result when ideally the augmented process noise covariance $Q_{a,d}$ equals to the real augmented process noise covariance, and the same for the measurement noise covariance R_d. Whether from the deterministic or the stochastic point of view, reducing the magnitude of the elements in $Q_{a,d}$, or increasing the magnitude of the elements in R_d informs the UKF so that it is adapted to the situation for which the measurement noise is important compared to the augmented process noise. As a result, the UKF will give more confidence or weight to the augmented state transition model than to measurements. The Kalman gain matrix will have reduced value components focusing more on the augmented state predictions and less on measurement corrections (Dutton et al., 1997). Under this condition, the augmented state reconstruction dynamics will be slow (low correction level from the measurements) but will be more weakly impacted by a worse measurement quality. On the contrary, i.e. by assuming *a priori* that the measurement noise is lower compared to augmented process noise, the augmented system states reconstruction will be faster but also more sensitive to the quality of the measurements.

To study the parameter evolution in driver's adaptation process, the initial augmented states value $\hat{x}_a[0]$ and states covariance $P_a[0]$ are not quite important. We focus mainly on

the tuning of matrix $Q_{a,d}$ and R_d. A simple and intuitive choice is that $Q_{a,d}$ is block-diagonal, i.e.

$$Q_{a,d} = \begin{bmatrix} Q_{x,d} & 0 \\ 0 & Q_{\Theta,d} \end{bmatrix} \quad (12)$$

where $Q_{x,d}$ and $Q_{\Theta,d}$ are respectively the covariance matrices of the discretized states and parameters process noise. (12) means the following hypothesis is admitted:

Hypothesis 3: there is no correlation within the process noise between system states and parameters.

In addition, for measurement noise:

Hypothesis 4: there is no correlation in measurements noise between system outputs, i.e. R_d is diagonal.

One of the difficulties in applying the aforementioned tuning rules (confidence on measurements versus states evolution) to define the magnitude of the elements of the matrix $Q_{a,d}$ and R_d comes from its qualitative nature. Normalization is required because the signals can be very diverse, concerning their range of amplitude values, but also their impact on states and output signals. On one side, for output signals with scattered ranges of variation, it is important to *a priori* normalize measurement noise properly accordingly, by adequate choice in R_d (see (13)). On the other side, the process noise may be normalized through its effects on the system outputs. These effects may be evaluated through using the observability Gramian for $Q_{x,d}$ tuning, as proposed in (de Larminat, 2009) for setting a Kalman Filter with a homogenized observer dynamics. It is more easily derived for $Q_{\Theta,d}$ tuning from the parametric sensitivity of the output. In this case, normalization from the nominal value of the parameters is possible and will be considered to simplify presentation. Algorithm 3 details the UKF tuning process.

Algorithm 3: Tuning UKF

Step 1: Choose R_d

Given outputs data $y[k]$ on $k \in [0, N]$ with dimension M, supposing each output has an error ratio of σ_i (inverse of the confidence level as stated above), R_d is

$$R_d = diag\left(\sigma_i^2 y_{i,max}^2\right), i = 1,2,\dots,M \quad (13)$$

where $y_{i,max} = \max_{k\in[1,N]} |y_i[k]|$.

Step 2: Normalize $Q_{x,d}$

Given (2) with parameters fixed at normal values in Table 2 as a normal LTI system, calculate the observability Gramian of the discretized normal LTI system

$$G_o = \sum_{k=0}^{\infty} (A_d^T)^k C_d^T C_d A_d^k \quad (14)$$

Step 3: Choose $Q_{x,d}$

Choose a time scaling factor T_x so that $Q_{x,d} = [T_x G_o]^{-1}$ lead the LTI observer inherited from (2) (with nominal parameters) having its poles with real part less than $-1/T_x$.

Verification is possible by solving the adequate algebraic Riccati equation.

Step 4: Choose $Q_{\Theta,d}$

Choose an error ratio of α_i for each parameter and a time scaling factor T_Θ according to the Hypothesis 2:

$$Q_{\Theta,d} = \frac{1}{T_\Theta} diag\left(\alpha_i^2 \Theta_{i,nom}^2\right), i = 1,2,\dots,P \quad (15)$$

where $\Theta_{i,nom}$ is the nominal value of ith parameter.

4.2 Multi-UKF Approach

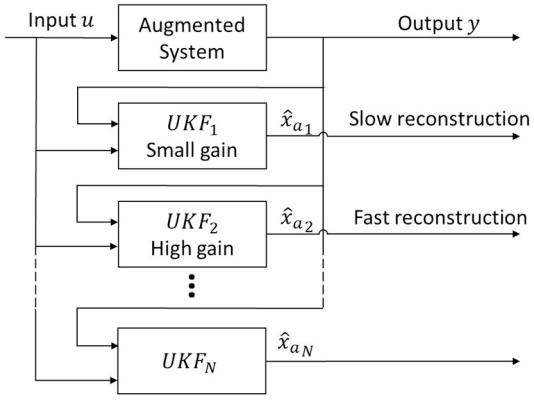

Fig. 2 Multi-UKF schema

As the result of such a tuning is always a compromise between rapidity and precision (noise sensitivity) in the process of parameters estimation, a multi-model UKF based approach is considered. At least two UKF will be used (see Fig. 2). One is configured to get a precise steady-state value of the parameters considered. The other is configured to detect possible fast variations.

5. EXPERIMENTS

The identification method as well as the tuning methodology are validated by two experiments: one in Simulink© and one on the driving simulator SCANeR©. In these experiments, the cybernetic driver model (2) is utilized as a virtual driver. Some of its parameters are *a priori* increased gradually at different times. In this case study, the increase of both visual gains (K_p and K_c) may depict increasing stress in driver's mind, or weak visibility conditions (like foggy or dark). The experiment steps are the following: the virtual driver steers a vehicle on a predefined road; the parameters change during driving; inputs and outputs data are collected; the data is used to identify the augmented system states including the searched parameters. The main differences between the two experimental platforms are: on the driving simulator 1) the vehicle is more realistic and precise, 2) the vehicle is controlled by a real steering column instead of a mathematical model and 3) some inputs and outputs data are collected by sensors. Besides, the multi-UKF approach is used in the second experiment so as to evaluate the tuning methodology.

5.1 Experiment in Simulink©

The first experiment is realized by simulating a Driver-Vehicle-Road (DVR) model (Saleh et al., 2013) in Matlab / Simulink©. The simulation environment (see Fig. 3) was

established in previous researches. The vehicle-road (VR) model is a bicycle model of which parameters were identified from experimental data. The cybernetic driver model "steers" the VR model with a fixed speed 64 km/h on a predefined road (see Fig. 4).

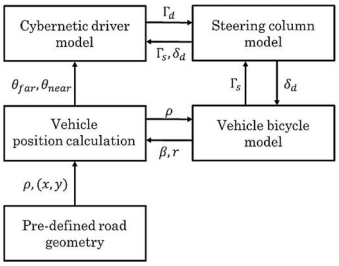

Fig. 3 Models in Simulink©

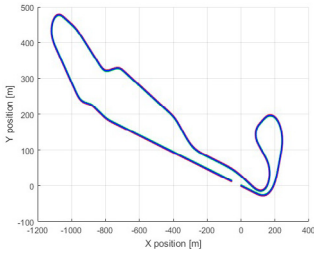

Fig. 4 Road in Matlab©

Three different situations are simulated in this experiment: 1) only K_p increases; 2) only K_c increases; and 3) both K_p and K_c increase. A small gain UKF is implemented in all situations, of which the configuration could be found in (16), (17), (18) and (19). The identification results are shown respectively in Fig. 5, 6 and 7. The red solid line is the actual variation of parameters during simulation, the blue dashed line is the estimated variation of parameters and the yellow dotted line represents for the related input signals (θ_{far} for K_p, θ_{near} for K_c, see Fig. 1).

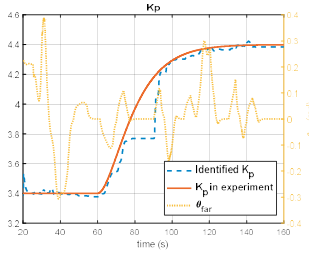

Fig. 5 Only K_p increases

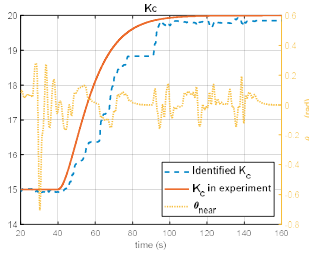

Fig. 6 Only K_c increases

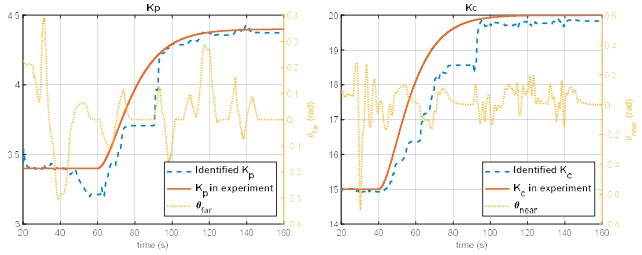

Fig. 7 Both K_p and K_c increase

Several observations could be obtained from these figures. Firstly, the results prove the feasibility of the identification method in tracing variation of parameters. Secondly, as long as the related input signal becomes "weak", i.e. the input excitation is low, the corresponding parameter keeps constant due to "weak" identifiability. For example, in Fig. 5 from 80s to 90s, the input signal θ_{far} is almost 0, in the meantime the identified K_p is constant. Same in the Fig. 6 for θ_{near} and the identified K_c during 80s and 90s. The reason of "weak" input signals here is trivial: the "driver" is driving on a straight road. Thirdly, in Fig. 7 the variation of the identified K_p is different from that in Fig. 5 during 40s to 60s, this is caused by the correlation between two parameters, since K_c starts changing at 40s.

5.2 Experiment on SCANeR©

The second experiment is realized on the driving simulator SCANeR© (see Fig. 8), where researches on human driver's adaptation will take place afterwards. It is equipped with a complete dashboard, a common five-speed gear stick, pedals of gas, brake and clutch, and a TRW direction system with steering wheel. The visual scene is displayed on 3 LCD screens, a central one in front of driver and two others oriented to the centre one with 45°. They cover a field of view of 25° on height and 115° on width. The visual scene transmits the road characteristics as perceived by driver via the windshield. A small family car of type Peugeot 307 is chosen as vehicle model in this experiment. The driver model also "steers" the vehicle with a fixed speed 64 km/h on a predefined road (see Fig. 9). Both parameters, K_p and K_c, are supposed to change.

Fig. 8 Driving simulator SCANeR©

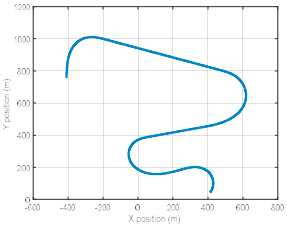

Fig. 9 Experiment road in the driving simulator

The multi-UKF approach with two different configurations of UKF is used to identify the parameter evolution. In both UKFs, the value for initial system states are simply 0, while the estimated parameters are initialized without error to the initial values (see Table 2) used for the simulation.

$$\hat{x}_a[0] = [0 \quad 0 \quad 0 \quad 3.4 \quad 15]^T \tag{16}$$

The initial augmented system state covariance $P_a[0]$ is chosen arbitrarily as stated in section 4.1.The UKFs are now tuned according to Algorithm 3:

$$R_d = diag(9 \times 10^{-4}, 25 \times 10^{-4}) \tag{17}$$

$$Q_{x,d} = 10^{-7} \times G_o^{-1} \tag{18}$$

This tuning leads to poles at: -1, -10 and -50 meaning that the slowest dynamics of observer will have a time constant of 1 second, which seems sufficient. In fact, the state observer in open-loop is fast enough.

Finally, different tuning are made for $Q_{\Theta,d}$ to get the two UKF. For UKF1:

$$Q_{\Theta,d} = 10^{-8} \times diag(3.4^2, 15^2) \tag{19}$$

The scaling factor in $Q_{\Theta,d}$ is modified for UKF2:

$$Q_{\Theta,d} = 10^{-6} \times diag(3.4^2, 15^2) \tag{20}$$

The results are shown respectively in Fig. 10 and Fig. 11. Same as in the first experiment, identified parameters are constant when "weak" identifiability happens. In addition, compared

with Fig. 10, the constant values are greater in Fig. 11. For example K_c is almost constant from 40s to 60s, while its value is about 15.5 in Fig. 10 and 16 in Fig. 11. This proves the rapidity of the UKF2. Besides, the results of UKF2 are more sensible to noise, this is obvious on the figures during 120s to 160s. It should be noted that K_c has an undesired variation from 80s to 110s in UKF1. Although the estimations eventually converge, there is also some slowness for UKF2 between 120s and 180s for K_p.

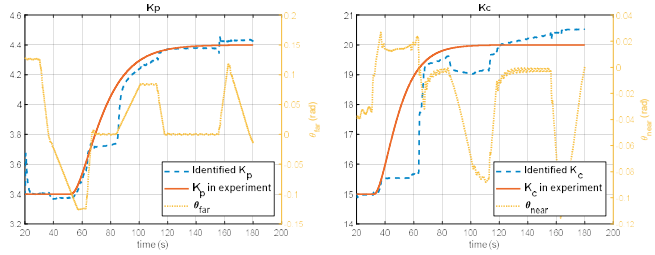

Fig. 10 Results of the UKF1 with slow reconstruction

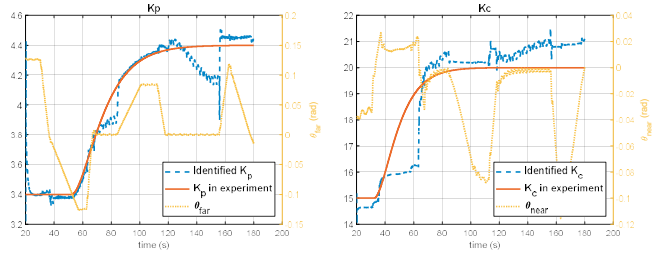

Fig. 11 Results of the UKF2 with fast reconstruction

6. CONCLUSION

This article shows the interest and the feasibility of tracking the variations of parameters related in particular to the visual part of a driver model, so called cybernetic driver model. This problem is essential to study the adaptation of the driver's behaviour to different changes in his driving environment, e.g. adaptation to active steering control systems, road features or meteorology. The driver model chosen is based on knowledge concerning neurophysiology and psychology of human driver, useful to study the driver's adaptation. The LPV identification problem was solved by first augmenting LPV system states with the state-space differential equations characterizing parameters' evolution dynamics. Then the Unscented Kalman Filter was applied by considering the identification problem as a state estimation problem. Referring to methodological experiences concerning classical Kalman Filter, the tuning of UKF was mainly accomplished by setting the parameters' process and measurement noise covariance matrices. The compromise between rapidity and precision of parameter estimation was discussed through considering a multi-UKF approach. One UKF estimates the mean value of parameters while another one makes it possible to detect fast parametric variations. Two experiments considering a sequential change of parameters showed good identification results, compatible with the aim (driver adaptation analysis). However, a coupling effect may appear especially if the UKF is configured for high dynamic performance. Nevertheless, although this effect still needs to be understood more in depth from a theoretical point of view, the identification method considered (multi-UKF approach) proved to be useful in the future, for investigating especially the adaptation of human driver to the driver-assistance systems.

Extensive tests will now be performed on the LS2N driving simulator, with a significant number of human drivers. We believe that the proposed methodology will allow us to better understand driver's adaptive dynamics over time.

ACKNOWLEDGEMENT

This work was supported by RFI Atlanstic 2020, funded by the Region Pays de la Loire.

REFERENCES

Abbink, D. A., Mulder, M., & Boer, E. R. (2012). Haptic shared control: Smoothly shifting control authority? *Cognition, Technology and Work*, *14*(1), 19–28.

Ameyoe, A., Chevrel, P., Le-Carpentier, E., Mars, F., & Illy, H. (2015). Identification of a Linear Parameter Varying Driver Model for the Detection of Distraction. *1st IFAC Workshop on Linear Parameter Varying Systems LPVS 2015*, *48*(26), 37–42.

Darwish, M. A. H., Cox, P. B., Proimadis, I., Pillonetto, G., & Tóth, R. (2018). Prediction-error identification of LPV systems: A nonparametric Gaussian regression approach. *Automatica*, *97*, 92–103.

de Larminat, P. (2009). *Automatique Appliquée* (2nd ed.). Paris: LAVOISIER.

Donges, E. (1978). A Two-Level Model of Driver Steering Behavior. *Human Factors: The Journal of the Human Factors and Ergonomics Society*, *20*(6), 691–707.

Dutton, K., Thompson, S., & Barraclough, B. (1997). The Kalman filter. In *The art of control engineering* (3rd ed., pp. 484–492). Addison Wesley.

Flad, M., Frohlich, L., & Hohmann, S. (2017). Cooperative shared control driver assistance systems based on motion primitives and differential games. *IEEE Transactions on Human-Machine Systems*, *47*(5), 711–722.

Hess, R. A., & Modjtahedzadeh, A. (1990). A Control Theoretic Model of Driver Steering Behavior. *IEEE Control Systems Magazine*, *10*(5), 3–8.

Hoult, W., & Cole, D. J. (2008). A neuromuscular model featuring co-activation for use in driver simulation. *Vehicle System Dynamics*, *46*(sup1), 175–189.

Julier, S. J., & Uhlmann, J. K. (1997). New extension of the Kalman filter to nonlinear systems. *Proc. SPIE 3068,Signal Processing, Sensor Fusion, and Target Recognition VI*. https://doi.org/10.1117/12.280797

Mars, F., & Chevrel, P. (2017). Modelling human control of steering for the design of advanced driver assistance systems. *Annual Reviews in Control*, *44*(Supplement C), 292–302.

Mars, F., Deroo, M., & Charron, C. (2014). Driver adaptation to haptic shared control of the steering wheel.

Proceedings of the 2014 IEEE International Conference on Systems, Man and Cybernetics, 1524–1528.

Mars, F., Deroo, M., & Hoc, J. M. (2014). Analysis of human-machine cooperation when driving with different degrees of haptic shared control. *IEEE Transactions on Haptics*, *7*(3), 324–333.

Mars, F., Saleh, L., Chevrel, P., Claveau, F., & Lafay, J.-F. (2011). Modeling the visual and motor control of steering with an eye to shared-control automation. *Human Factors and Ergonomics Society 55th Annual Meeting*, *55*, 1422–1426. Las Vegas, United States.

McRuer, D. T., Allen, R. W., Weir, D. H., & Klein, R. H. (1977). New Results in Driver Steering Control Models. *Human Factors: The Journal of the Human Factors and Ergonomics Society*, *19*(4), 381–397.

Mole, C., Lappi, O., Giles, O., Markkula, G., Mars, F., & Wilkie, R. (2019). Getting Back Into the Loop: The Perceptual-Motor Determinants of Successful Transitions out of Automated Driving. *Human Factors The Journal of the Human Factors and Ergonomics Society*. https://doi.org/10.1177/0018720819829594

Mulder, Mark, Abbink, D. A., & Boer, E. R. (2012). Sharing control with haptics: Seamless driver support from manual to automatic control. *Human Factors*, *54*(5), 786–798.

Mulder, Max, Van Paassen, M. M., & Boer, E. R. (2004). Exploring the roles of information in the manual control of vehicular locomotion: From kinematics and dynamics to cybernetics. *Presence: Teleoperators and Virtual Environments*, *13*(5), 535–548.

Rizvi, S. Z., Velni, J. M., Abbasi, F., Tóth, R., & Meskin, N. (2018). State-space LPV model identification using kernelized machine learning. *Automatica*, *88*, 38–47.

Saleh, L., Chevrel, P., Claveau, F., Lafay, J. F., & Mars, F. (2013). Shared steering control between a driver and an automation: Stability in the presence of driver behavior uncertainty. *IEEE Transactions on Intelligent Transportation Systems*, *14*, 974–983.

Saleh, L., Chevrel, P., Mars, F., Lafay, J. F., & Claveau, F. (2011). Human-like cybernetic driver model for lane keeping. *Proceedings of the 18th IFAC World Congress*, 4368–4373.

Salvucci, D. D., & Gray, R. (2004). A two-point visual control model of steering. *Perception*, *33*(10), 1233–1248.

Steele, M., & Gillespie, R. B. (2001). Shared Control between Human and Machine: Using a Haptic Steering Wheel to Aid in Land Vehicle Guidance. *Proceedings of the Human Factors and Ergonomics Society Annual Meeting*, *45*(23), 1671–1675.

Tóth, R., Laurain, V., Gilson, M., & Garnier, H. (2011). On the closed loop identification of LPV models using instrumental variables. *18th IFAC World Congress*, *44*(1), 7773–7778.

Wan, E. A., van der Merwe, R., & Nelson, A. T. (2000). Dual estimation and the unscented transformation. *Advances in Neural Information Processing Systems*, 666–672.

Zhang, Q., & Ljung, L. (2017). From structurally independent local LTI models to LPV model. *Automatica*, *84*, 232–235.